BIOLOGY OF REPRODUCTION **69,** 2059–2067 (2003)
Published online before print 20 August 2003.
DOI 10.1095/biolreprod.103.020537

Distinctions in Meiotic Spindle Structure and Assembly During In Vitro and In Vivo Maturation of Mouse Oocytes[1]

Alexandra Sanfins,[2,3,4] Gloria Y. Lee,[3] Carlos E. Plancha,[4] Eric W. Overstrom,[5] and David F. Albertini[3]

Department of Anatomy and Cellular Biology,[3] Tufts University School of Medicine, Boston, Massachusetts 02111
Unidade de Biologia da Reprodução,[4] Faculdade de Medicina de Lisboa, Lisboa, Portugal
Department of Biomedical Sciences,[5] Tufts University School of Veterinary Medicine, Grafton, Massachusetts 01536

ABSTRACT

To better understand the differences in cytoskeletal organization between in vivo (IVO) and in vitro (IVM) matured oocytes, we analyzed remodeling of the centrosome-microtubule complex in IVO and IVM mouse oocytes. Fluorescence imaging revealed dramatic differences in meiotic spindle assembly and organization between these two populations. Metaphase spindles at both meiosis I (M-I) and meiosis II (M-II) in IVO oocytes were compact, displayed focused spindle poles with distinct γ-tubulin foci, and were composed of acetylated microtubules. In contrast, IVM oocytes exhibited barrel-shaped spindles with fewer acetylated microtubules and γ-tubulin diffusely distributed throughout the spindle proper. With respect to meiotic progression, IVO oocytes were more synchronous in the rate and extent of anaphase to telophase of M-I and first polar body emission than were IVM counterparts. Furthermore, IVO oocytes showed a twofold increase in cytoplasmic microtubule organizing centers (MTOCs), and constitutive MTOC proteins (γ-tubulin and pericentrin) were excluded from the first polar body. Inclusion of MTOC constitutive proteins in the polar body and diminished number of cytoplasmic MTOCs was observed in IVM oocytes. These findings were corroborated in IVO oocytes obtained from naturally ovulated and spontaneously cycling mice and highlight a fundamental distinction in the spatial and temporal regulation of microtubule dynamics between IVO and IVM oocytes

assisted reproductive technology, meiosis, oocyte development

INTRODUCTION

Mechanisms marshaled during the pre- and periovulatory stages of ovarian follicle development generally result in the production of ova that are capable of supporting embryonic development in mammals. Ova produced during natural or induced ovulation are mature with respect to their nuclear and cytoplasmic status, and in many mammals, their developmental competence is likely to be superior to that of oocytes that have matured ex vivo [1–4]. Since the original discovery that mammalian oocytes will spontaneously resume and complete meiosis upon removal from the follicle [5, 6], much effort has been expended to modify culture conditions for in vitro maturation (IVM) in an effort to obtain higher quality oocytes for embryo production [7, 8]. In some mammals, such as cattle, IVM represents the industry standard and is routinely used for in vitro fertilization or nuclear transfer and embryo production strategies and results in relatively high rates of blastocyst development and implantation [9, 10]. Yet, despite the successes in producing live young from IVM oocytes in other mammals, including humans, it is evident that the distinguishing features of in vivo matured (IVO) oocytes that confer greater developmental potential remain obscure [11]. From a practical point of view, constructive efforts to optimize clinical IVM will require evidence of successful embryonic development and identification of oocyte markers that predict successful nuclear and cytoplasmic maturation.

Extrusion of the first polar body (PB) as meiosis I (M-I) is completed remains a benchmark for evaluation of IVM oocytes even though this process can be experimentally uncoupled from karyokinesis in mice and hamsters [12, 13] and fails to reveal underlying cell cycle aberrations during IVM of human and hamster oocytes [13, 14]. With mounting evidence suggesting that cytoplasmic quality in IVO mouse oocytes plays a major role in determining embryonic potential [15, 16], it is imperative that discriminating analyses of IVO and IVM oocytes be undertaken to obtain much needed insight into the major metabolic and structural determinants that could account for oocyte quality.

The goal of the present studies was to evaluate properties of meiotic spindle and cytoplasmic microtubules (MTs) in mouse oocytes matured under IVO or IVM conditions. Our results indicate that spatial and temporal parameters of oocyte maturation are significantly different with respect to the recruitment and stabilization of the centrosome-MT complex. Although these findings may be related or even account for the well-known developmental competence differences between IVO and IVM oocytes, clear support for this hypothesis waits further studies. However, these findings are relevant for optimizing conditions for IVM and point to underlying factors that should be taken in consideration when studying the origins of chromosomal aneuploidies or other developmental defects observed during the use of human assisted reproductive technologies (ARTs) [17, 18].

MATERIALS AND METHODS

Collection and Culture of Mouse Oocytes

All experiments were performed using 6- to 10-wk-old CF-1 mice (Charles River). Animals were handled according to the *Guide for Care and Use of Laboratory Animals* (National Academy of Science, 1996) and

[1]This work was supported by grants from Fundaçao para a Ciencia e Tecnologia SFRH/BD/2757/2000 (to A.S.), POCTI/ESP/43628/2000 (to C.E.P.), March of Dimes Birth Defects Foundation 01-248 (to D.A.), and USDA-NRI 2001-35203-09966 (to E.O. and D.A.).
[2]Correspondence: Alexandra Sanfins, Department of Anatomy and Cellular Biology, Tufts University School of Medicine, 136 Harrison Ave., Boston, Massachusetts 02111. FAX: 617 636 6536; e-mail: alexa_sanfins@yahoo.com

Received: 21 June 2003.
First decision: 16 July 2003.
Accepted: 14 August 2003.

ISSN: 0006-3363. http://www.biolreprod.org

were maintained at a 14L:10D photoperiod under constant temperature and relative humidity conditions. Food and water were provided ad libitum. Naturally ovulated oocytes (IVO-N) were collected from cycling animals. Estrous cycle was evaluated daily by visual examination of the vagina [19], and the condition was confirmed by examination of vaginal smears [29]. Mice in estrus were killed, and cumulus-oocyte masses were recovered from the ampulla into collection medium consisting of Hepes-buffered Eagle minimal essential medium (MEM) with Hanks salts supplemented with 100 IU/ml penicillin, 100 μg/ml streptomycin, and 0.3% BSA. Following removal of cumulus cells by brief treatment with hyaluronidase (190 IU/ml; Sigma, St. Louis, MO) for 5 min at room temperature, oocytes were immediately fixed and extracted for 30 min at 37°C in an MT stabilizing buffer (0.1 M PIPES, pH 6.9, 5 mM $MgCl_2 \cdot 6H_2O$, 2.5 mM EGTA) containing 2% formaldehyde, 0.1% Triton X-100, 1 mM taxol, 10 units/ml aproptinin, and 50% deuterium oxide [20]. Oocytes were stored at 4°C until further processing in a blocking solution of PBS containing 2% BSA, 2% powdered milk, 2% normal goat serum, 0.1 M glycine, and 0.01% Triton X-100. IVO oocytes were obtained from mice previously injected with 5 IU eCG (Sigma) to stimulate follicular development followed 47 h later by 5 IU hCG (Sigma) to induce ovulation. Oocytes were collected from preovulatory Graafian follicles (at 4, 6, 8, and 10 h post-hCG) or in the oviducts at 12 and 14 h post-hCG. Following removal of cumulus cells by brief treatment with hyaluronidase, oocytes were immediately fixed and stored until processing. For IVM experiments, mice were injected 47 h earlier with 5 IU of eCG, and cumulus-enclosed oocytes were collected by follicular puncture in collection medium and either immediately fixed or cultured for 4, 6, 8, 10, 12, and 14 h in IVM medium (basal IVM medium) consisting of Eagle MEM supplemented with Earle salts, 2 mM glutamine, 0.23 mM pyruvate, 100 IU/ml penicillin, 100 μg/ml streptomycin, and 0.3% BSA in a humidified atmosphere of 5% CO_2 in air. After removing the cumulus cells by gentle pipetting, oocytes were fixed and stored at 4°C until further processing.

Processing of Oocytes for Fluorescence Microscopy

IVM (n = 560), IVO (n = 1444), and IVO-N (n = 43) oocytes were processed in parallel for fluorescence microscopy to assess chromatin, MTs, γ-tubulin, pericentrin, and mitotic phosphoprotein (MPM-2) organization. Oocytes were incubated with a sequential order of primary and secondary antibodies. Labeling strategies were such that each group of oocytes was separately processed for MPM-2 (mouse) followed by anti-mouse secondary, α-tubulin (rat), and anti-rat secondary. This sequence was followed for γ-tubulin (mouse) and α-tubulin (rat); acetylated-tubulin (mouse) and α-tubulin (rat); pericentrin (rabbit) and α-tubulin (rat). Each antibody was incubated for 1 h at 37°C with shaking followed by three 15-min washes in blocking solution. Labeling pairs in sequence were a) MPM-2 mouse monoclonal (1:100 dilution; Upstate Biotechnology, Lake Placid, NY) followed by a 1:100 dilution of affinity-purified fluoresceinated donkey anti-mouse IgG (Jackson Laboratories, Bar Harbor, ME), b) mouse monoclonal anti-γ-tubulin (1:100 dilution; Sigma) followed by a 1:100 dilution of Cy-3 donkey anti-mouse IgG (Jackson Laboratories), c) mouse monoclonal anti-acetylated tubulin (1:100; Sigma) followed by Cy-3 donkey anti-mouse IgG (Jackson Laboratories), and d) IVO-N oocytes were labeled for pericentrin using a polyclonal anti-pericentrin (Covance, Berkeley, CA) followed by Alexa-fluor 568 goat anti-rabbit IgG (1:800; Molecular Probes, Eugene, OR). All samples were subsequently stained with a 1:200 dilution of the rat monoclonal antibody to α-tubulin YOL-34 [21] with appropriate secondary antibody, namely for a) Cy-3 donkey anti-rat IgG (Jackson Laboratories) and for b), c), and d) 1:100 dilution of affinity-purified fluoresceinated donkey anti-rat IgG. Oocytes were mounted under the same conditions using 1.5 μl of a 50% glycerol/PBS solution containing sodium azide and Hoechst 33258 (1 μg/ml; Polysciences, Warrington, PA) to label chromatin. Incubation of oocytes in secondary antibodies alone failed to yield detectable staining both singly or in repeat sequence as above. Labeled oocytes were analyzed using an IM-35 inverted microscope (Zeiss, Thornwood, NY) and a 50-W mercury arc lamp using 40× and 63× Neofluor objectives. Digital images were collected with a Orca ER digital camera (model C4742-95; Hamamatsu Corp., Bridgewater, NJ) interfaced with a Meta Morph Imaging System (Universal Imagine Corp., Downington, PA). A triple band pass dichroic and automated excitation filter selection permitted collection of in-frame images with minimal magnification or spatial distortion.

Spindle Measurements, Cytoplasmic MT Organizing Center Quantification, and Statistical Analysis

Digital images were obtained with integration times of 300–600 msec for each fluor channel at subsaturation pixel intensities, and thresholding and measurements were done with Meta Morph Imaging System 5.0. All size measurements were based on image scaling after distances were calculated using stored images of a micrometer scale under identical magnification conditions. Because of visible asymmetry in the meiotic spindles, a formula was derived for determination of spindle area that would take into account differences between each half-spindle. Figure 1 depicts in diagrammatic form (not to scale) the two extremes in spindle shape encountered and values recorded for spindle length (h) and width at each pole (a, b) and the spindle equator (c). Images with clear definition of spindle organization were analyzed from a minimum of 30 oocytes in each category (M-I and M-II in IVM, IVO, and IVO-N oocytes). Measurements of meiotic M-I and M-II spindle areas and mean width of M-I and M-II spindle poles for IVM, IVO, and IVO-N oocytes were compared and the number of cytoplasmic MT organizing centers (MTOCs) was quantified by focusing through the entire oocyte volume. Analysis of spindle measurements (total area and spindle pole width) and number of cytoplasmic MTOCs were represented by notched box and whisker plots (Slide Write Plus for Windows, Version 5.01; Advanced Graphics Software Inc., Encinitas, CA). Notched box plots display order statistics, and the notches of the box plots correspond to median confidence limits. Statistically, two medians are considered significantly different at the 0.05 level if their confidence limits do not overlap. Additionally, data were analyzed using SPSS 10.0 (Statistics Package for Social Sciences, Chicago, IL). Comparison of spindle areas and cytoplasmic MTOC numbers for each category of oocytes (M-I and M-II of IVO, IVO-N, and IVO) were evaluated using a nonparametric Kruskal-Wallis test followed by Mann-Whitney tests for two independent samples. Spindle pole widths were compared using one-way ANOVA followed by least significant difference and Tukey post hoc tests. Assumptions that the populations were normal (Shapiro-Wilk and Kolmogorov-Smirnov tests for normality) and population variances were all equal (Levene test) were checked prior to performing the ANOVA. If homogeneity of variances could not be assumed, a Tamhane post hoc test was used. Differences were considered significant at $P < 0.05$.

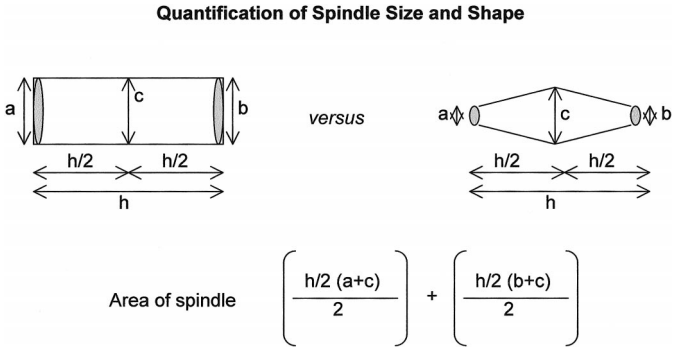

FIG. 1. Quantification of spindle size and shape. Two extreme spindle configurations evident in M-I or M-II mouse oocytes are depicted: flat-pole (barrel shape; left) and focused (tapered) pole (right). a, b, and c represent width measurements, and h represents total length. Formula for area incorporates all measures to obtain total area (μm^2) and accounts for variations in spindle symmetry from the equatorial axis.

RESULTS

Variations in Meiotic Spindle Shape and Size in Naturally Ovulated (IVO-N), Superovulated (IVO), and IVM Oocytes

Although previously published reports have indicating an anastral barrel-shaped meiotic spindle in M-II mouse oocytes [20, 22], our studies revealed clear and significant variations in spindle morphology with respect to the environment in which oocytes undergo meiotic maturation. We first examined M-II oocytes retrieved from mice undergoing natural estrous cycles (IVO-N). In all cases (n = 9 animals, 43 oocytes), M-II spindles were anastral and exhibited tapered poles where MTs were focused (Fig. 2). Spindle MTs were predominantly acetylated (Fig. 2A) and did not exhibit spatial overlap with polar MTOCs localized with antibodies to the constitutive centrosomal proteins γ-

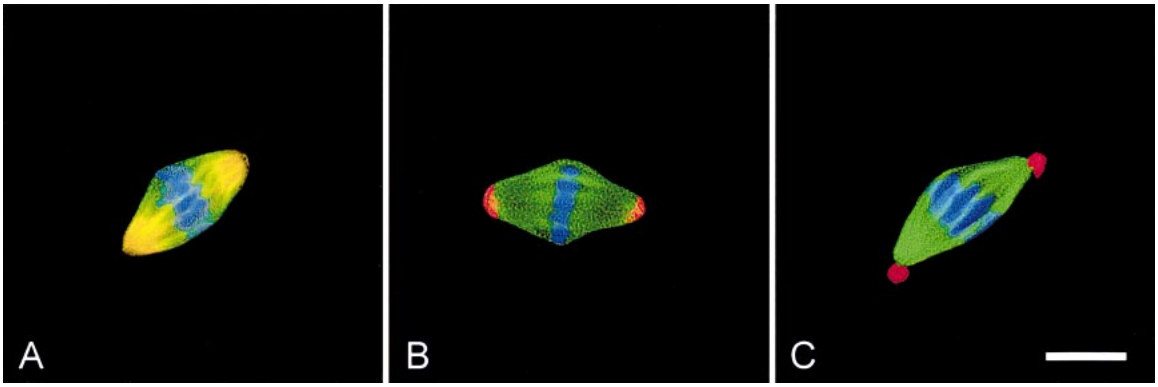

FIG. 2. Fluorescent images of naturally ovulated (IVO-N) metaphase II spindles of mouse oocytes labeled with total tubulin (green, **A**–**C**) and counterstained for acetylated tubulin (**A**), γ-tubulin (**B**), or pericentrin (**C**). Note superimposition of acetylated MTs with spindle MTs (**A**) converging at focused spindle poles. The centrosome markers γ-tubulin (**B**) and pericentrin (**C**) localize at the spindle poles. Bar equals 10 μm.

tubulin and pericentrin (Fig. 2, B and C). This finding in IVO-N oocytes of restricted localization of γ-tubulin to the poles and exclusion from the spindle prompted a more detailed study of spindle centrosome markers given recent studies on IVM mouse oocytes [12] and previous reports of the restricted localization of pericentrin in the same material [20, 23–25].

The distribution of spindle markers at M-I and M-II was consistently different in oocytes matured under IVO (n = 510) or IVM (n = 200) conditions (Fig. 3). For example, γ-tubulin was distributed throughout the spindle in M-I and M-II in IVM oocytes (Fig. 3, B and D) [12], whereas in IVO oocytes, γ-tubulin was clearly restricted to spindle pole foci (Fig. 3, A and C). In all cases and regardless of meiotic stage, IVM oocytes exhibited large barrel-shaped spindles with flat poles. Moreover, using markers for M-phase phosphoproteins (MPM-2) and MT acetylation, an indicator of MT stability [22] (Fig. 3, E–H and I–M, respectively), IVO oocytes exhibited distribution of these markers throughout the spindle proper (Fig. 3, E and G, and I and L, respectively), whereas IVM oocytes exhibited gaps in staining flanking the chromosomes of the metaphase plate, and staining was more concentrated toward the spindle poles (Fig. 3, F and H, and J and M, respectively). To ascertain more completely how maturation conditions affect the overall meiotic spindle structure, various parameters of spindle size and shape were analyzed.

Notched box plot analysis of IVO and IVM M-I spindles revealed a significant increase in spindle size based upon tubulin mass as evidenced in both the mean area (IVO M-I = 340 μm^2 vs. IVM M-I = 582 μm^2) and the overall range of areas observed within each group (IVO M-I = 204–637 μm^2 vs. IVM M-I = 246–1242 μm^2) (Fig. 4). The magnitude of spindle enlargement seen in M-II IVM oocytes was twofold more than that observed in M-II IVO spindles (IVO-M-II = 181 μm^2 vs. IVM M-II = 379 μm^2). A significant increase difference in spindle area was noted in M-I oocytes (71.2% increase in M-I vs. 109.3% increase in M-II), and a wider range of spindle area was noted at this stage possibly because of asynchrony in meiotic stage. M-II IVM oocytes exhibited a significant increase in spindle size when compared with both types of M-II IVO superovulated or naturally ovulated oocytes (IVM M-II = 379 μm^2 vs. IVO M-II = 181 μm^2 vs. IVO-N M-II = 148 μm^2). The spindle area of IVO M-II superovulated oocytes was statistically similar to that from naturally ovulated oocytes (IVO-N). Coupled with the selective staining patterns noted above, these data suggest that under IVM conditions mouse oocytes elaborate meiotic spindles that are larger in mass and lack distinct and restricted localization of markers related to MT nucleation (γ-tubulin) or stability (acetylation). Because the overall size and shape appeared to correspond to the disposition of spindle pole material, we next analyzed spindle pole width (Fig. 5). Again, spindle pole width was significantly greater in IVM oocytes at M-I (10.8 μm^2 vs. 6.6 μm^2 in IVO oocytes) or M-II (6.6 μm^2 vs. 4.0 μm^2), and in naturally ovulated oocytes there was even more striking diminution at both poles (2.9 μm^2). This finding is consistent with the observation that in general IVM oocytes exhibit expanded rings or C-shaped structures (Cs) denoted by pericentrin staining [20, 23, 24], and using γ-tubulin or pericentrin as markers of centrosomal integrity we have shown a more constricted focal mass of these proteins at the poles of IVO spindles (Figs. 2 and 3). To better understand how such differences in size and shape originate, we next examined the kinetics of meiotic progression and the overall pattern of spindle morphogenesis in IVO and IVM oocytes.

Kinetic Parameters of Meiotic Maturation Are Distinct in IVM and IVO Oocytes

Cumulus-enclosed oocytes were collected at 4, 6, 8, 10, 12, and 14 h following incubation in maturation medium (IVM) or following isolation from Graafian follicles of animals that had received hCG to induce ovulation (IVO). In four replicate experiments, IVM (n = 488) and IVO (n = 930) oocytes were evaluated for meiotic stages as described previously, and the percentage of oocytes at germinal vesicle breakdown (GVBD), M-I, anaphase I (A-I), telophase I (T-I), or M-II was determined in samples stained with Hoechst, total α-tubulin (YOL-34), acetylated-tubulin, MPM-2, or γ-tubulin. At 4 h, both IVO and IVM oocytes had undergone GVBD to the same extent (80%), indicating that the onset of M-phase resumption was similar under these conditions (Fig. 6). However, divergent patterns in both the rate and extent of meiotic progression were apparent in each group at subsequent times. Specifically, IVM oocytes exhibited prolonged GVBD and M-I stages from 4 to 10 h of culture, whereas in IVO oocytes GVBD stages were absent at 8 h, with the majority of oocytes at M-I by 8 h. A high degree of synchrony was evident in IVO oocytes; maximal incidence of M-I, A-I, and M-II were seen at 8, 10, and 12 h, respectively. In contrast, the broader distribution of IVM oocytes between these time points, coupled with a more delayed progression to M-II, all indicate

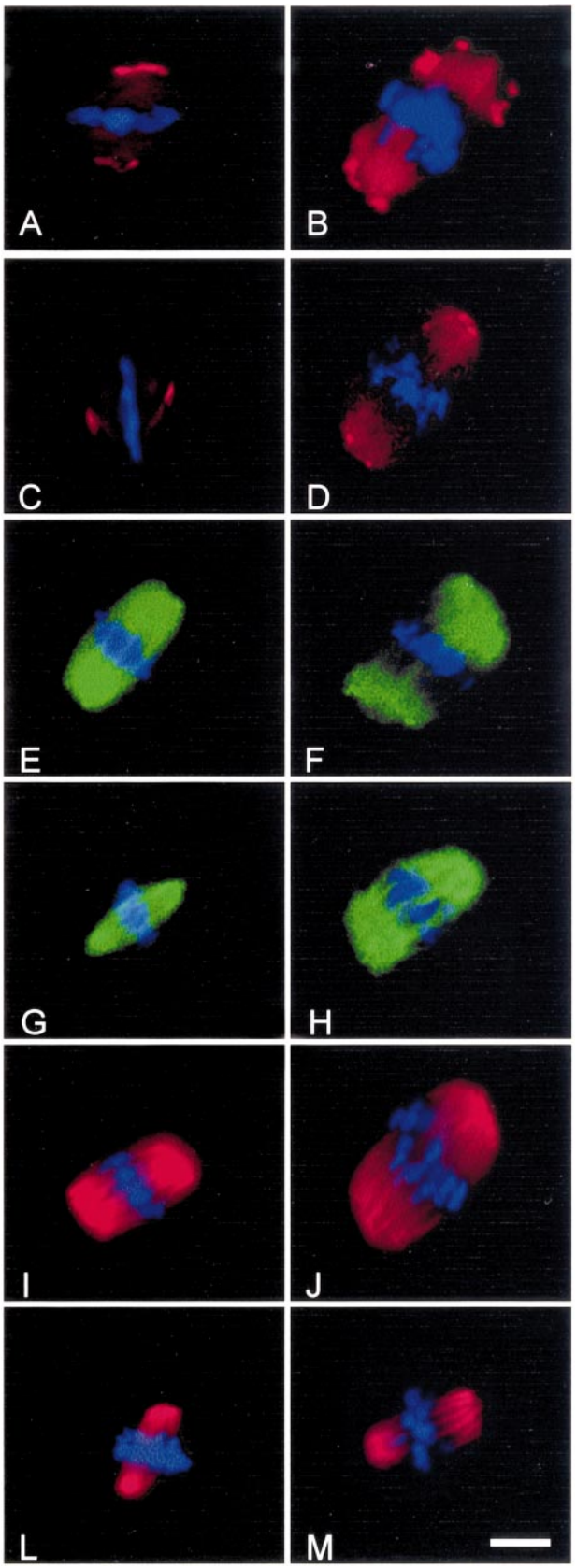

FIG. 3. Representative spindle images of IVO (left) and IVM (right) oocytes at M-I (**A**, **B**, **E**, **F**, **I**, and **J**) or M-II (**C**, **D**, **G**, **H**, **L**, and **M**) labeled with γ-tubulin (**A**–**D**), MPM-2 (**E**–**H**), and acetylated-tubulin. Note polar restriction and spindle proper absence of γ-tubulin in IVO oocytes (**A** and **C**) compared with IVM oocytes (**B** and **D**). Both MPM-2 and acetylated-tubulin (**I**–**M**) demonstrate that spindles of IVO oocytes are smaller and have more uniform distribution of epitope throughout spindle proper (**E**, **G**, **I**, and **L**) relative to IVM counterparts (**F**, **H**, **J**, and **M**). All magnifications are identical. Bar equals 10 μm.

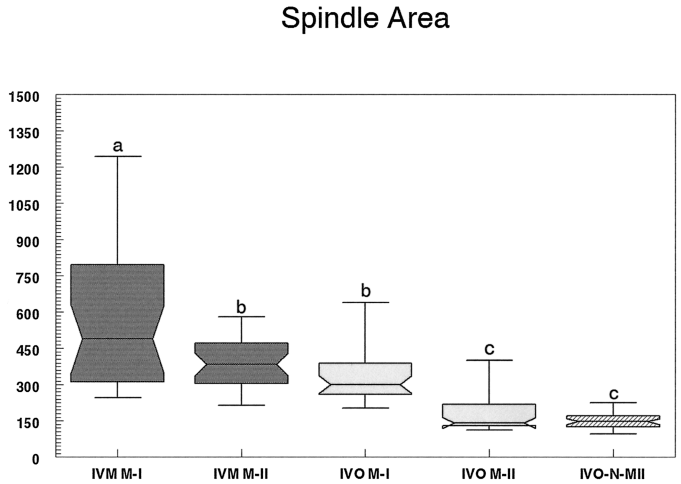

FIG. 4. Notched box plots of meiotic spindle areas for IVM or IVO oocytes in metaphase of M-I or M-II. For each represented meiotic stage (M-I and M-II), note the significant increase in spindle size and overall area range of IVM spindles when compared with spindles of superovulated (IVO) or naturally ovulated (IVO-N) oocytes based on tubulin mass. N represents numbers of spindles analyzed for each group. Different letters (a, b, and c) represent significant differences obtained across oocyte categories using nonparametric Kruskal-Wallis and Mann-Whitney tests ($P < 0.05$).

a less synchronous and somewhat delayed pattern of meiotic progression in IVM oocytes. Given these distinct meiotic progression parameters of rate and extent, we next examined the partitioning and redistribution of γ-tubulin because this protein is known to be a pivotal regulator of MT nucleation and any differences in its positioning might be involved in the overall timing and magnitude of spindle assembly.

Global and Local Patterns of γ-Tubulin Distribution in IVO and IVM Oocytes

Oocytes processed for the kinetic analysis described above were also evaluated to determine whether the smaller size of IVO oocyte spindles might be attributable to a more restricted redistribution of γ-tubulin during spindle formation. At 4, 6, and 8 h, we have noted three features of spindle morphogenesis that may be linked to the IVO versus IVM differences described. First, at 4 h the nuclear lamina-bound space in which condensed chromosomes are located, as previously reported by Combelles and Albertini [12], is more expanded in IVM oocytes than in IVO oocytes (Fig. 7, A and D, respectively). Whereas in IVM oocytes this domain is circumscribed by γ-tubulin aggregates of varying sizes (Fig. 7B), in IVO oocytes a solitary and eccentrically positioned plaque of γ-tubulin exists adjacent to a dominant cytoplasmic MTOC (Fig. 7E).

Notably, long MTs radially extend from this domain in prometaphase stages of both IVM and IVO oocytes, but at 6 h, as chromosome alignment proceeds (Fig. 7, G and J, respectively), chromosomes are straddled to two distinct spindle pole aggregates of γ-tubulin in IVO oocytes (Fig. 7L). In contrast, in IVM oocytes, a more diffuse MT-rich domain persists that remains outlined by γ-tubulin plaques (Fig. 7H). As spindle morphogenesis proceeds, a second

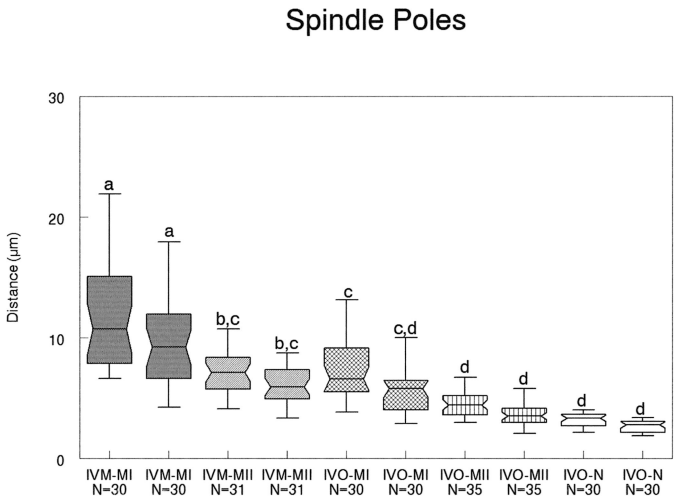

FIG. 5. Notched box plots of mean width of spindle poles taken from images of IVM or IVO oocytes at M-I or M-II and of IVO-N. Spindle pole width is significantly greater in IVM oocytes than in IVO oocytes at M-I or M-II. IVO-N oocytes exhibit striking constriction at both spindle poles. N represents numbers of spindles analyzed for each group. Different letters represent significant differences obtained across oocyte categories using a one-way ANOVA ($P < 0.05$).

major distinction is observed that involves γ-tubulin localization relative to the site of spindle MT assembly. At 8 h, in IVM oocytes strong staining for γ-tubulin is coincident with spindle fibers as the M-I spindle forms (Fig. 7, O and P), whereas in IVO oocytes a considerably reduced γ-tubulin signal overlies spindle MTs and the predominant location of γ-tubulin is seen within two distinct polar aggregates (Fig. 7, R and S). These findings suggest a more limited recruitment of γ-tubulin to the spindle assembly site in IVO oocytes and further suggest that the relatively greater exclusion of γ-tubulin from the lamina-bound chromosome domain may limit the number of MT nucleation events and therefore the final size of the meiotic spindle formed in IVO oocytes. Indications of restricted patterning and redistribution of pericentrin during IVM were also evident from an earlier analysis of the multiple cytoplasmic MTOCs known to be dynamically reorganized in mouse oocytes [20]. Therefore, we next analyzed the distribution and number of cytoplasmic MTOCs during M-I and M-II in IVM and IVO oocytes.

Cytoplasmic MTOCs contain pericentrin, γ-tubulin, MPM-2 epitope, and α-tubulin [20, 12] and typically undergo changes in MT nucleation that are cell-cycle stage specific [12]. Cytoplasmic MTOCs are partitioned and spatially separated from the forming spindle in both M-I and M-II oocytes occupying the spindle-lacking half of the oocyte, and at all stages examined these foci were positive for both γ-tubulin and α-tubulin. At both M-I and M-II stages, IVO and IVO-N oocytes contained twice the number of cytoplasmic MTOCs (Fig. 8; mean = 20 for IVO, 22 for IVO-N, 10 for IVM). Whether this doubling in density of similarly sized MTOCs reflects greater synthesis of precursors or immobilization of MTOCs in IVO that are more likely recruited to the spindle in IVMs remains unknown. Additionally, cytoplasmic MTOCs were excluded from the first PB of IVO and IVO-N oocytes but were present in the first PB of IVM oocytes (data not shown). This observation has also been reported by Ibanez et al. (in preparation) in a comparison between IVO and IVM oocytes from five distinct mouse strains.

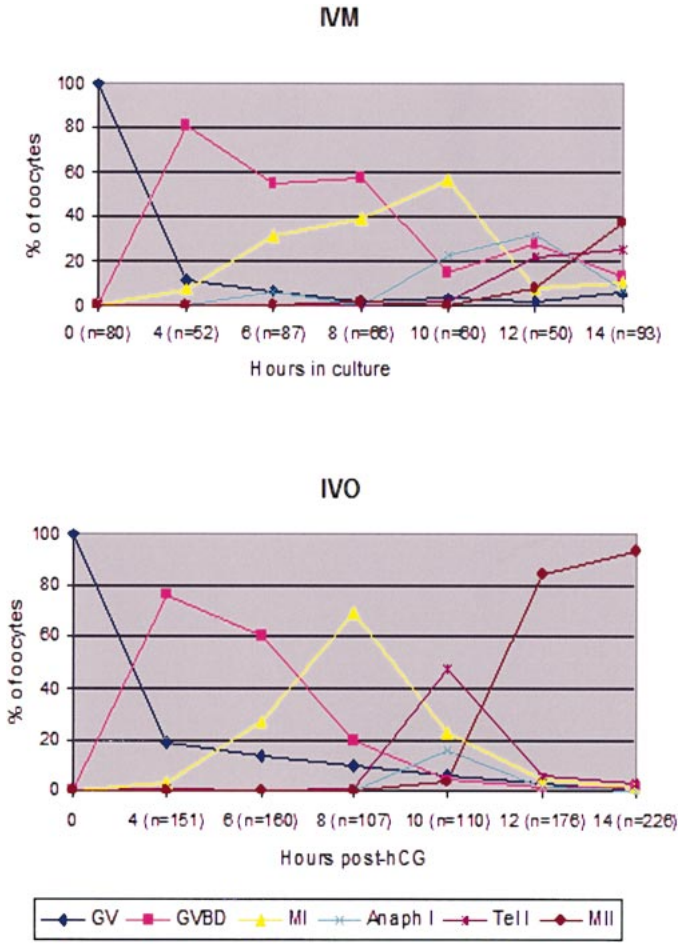

FIG. 6. Kinetics of meiotic progression in IVM or IVO oocytes. IVO oocytes exhibit a high degree of synchrony during meiotic progression when compared with IVM oocytes. Note the delayed pattern of meiotic progression in IVM oocytes. N represents number of oocytes analyzed at each time point.

DISCUSSION

Given the apparent differences in developmental potential exhibited by IVO and IVM oocytes in various mammals [1, 3, 4, 26] and the role of spindle positioning in the establishment of egg polarity [27], we asked whether conditions of meiotic maturation influence the reorganization of the MT cytoskeleton in mouse oocytes [28]. Our data have revealed several important differences between mouse oocytes that have been matured in response to a natural or induced LH surge or matured ex vivo. With respect to the meiotic spindle, the shape, density, and stability of MTs and disposition of γ-tubulin differed among these oocyte populations. In addition, the more synchronous pattern of meiotic progression coupled with the global retention of cytoplasmic MTOCs, their exclusion from the first PB, and diminished recruitment of γ-tubulin to the nascent spindle all point to a more conserved utilization of γ-tubulin during the critical events of meiotic maturation in IVO oocytes. Although these findings may be related to or partially account for developmental competence differences known to exist between IVM and IVO oocytes, a clear demonstration of this relationship requires further studies. Our results do however reveal profound differences in the centrosome-MT organization between these two oocyte populations and should be taken in consideration as potential biomarkers for oocyte quality.

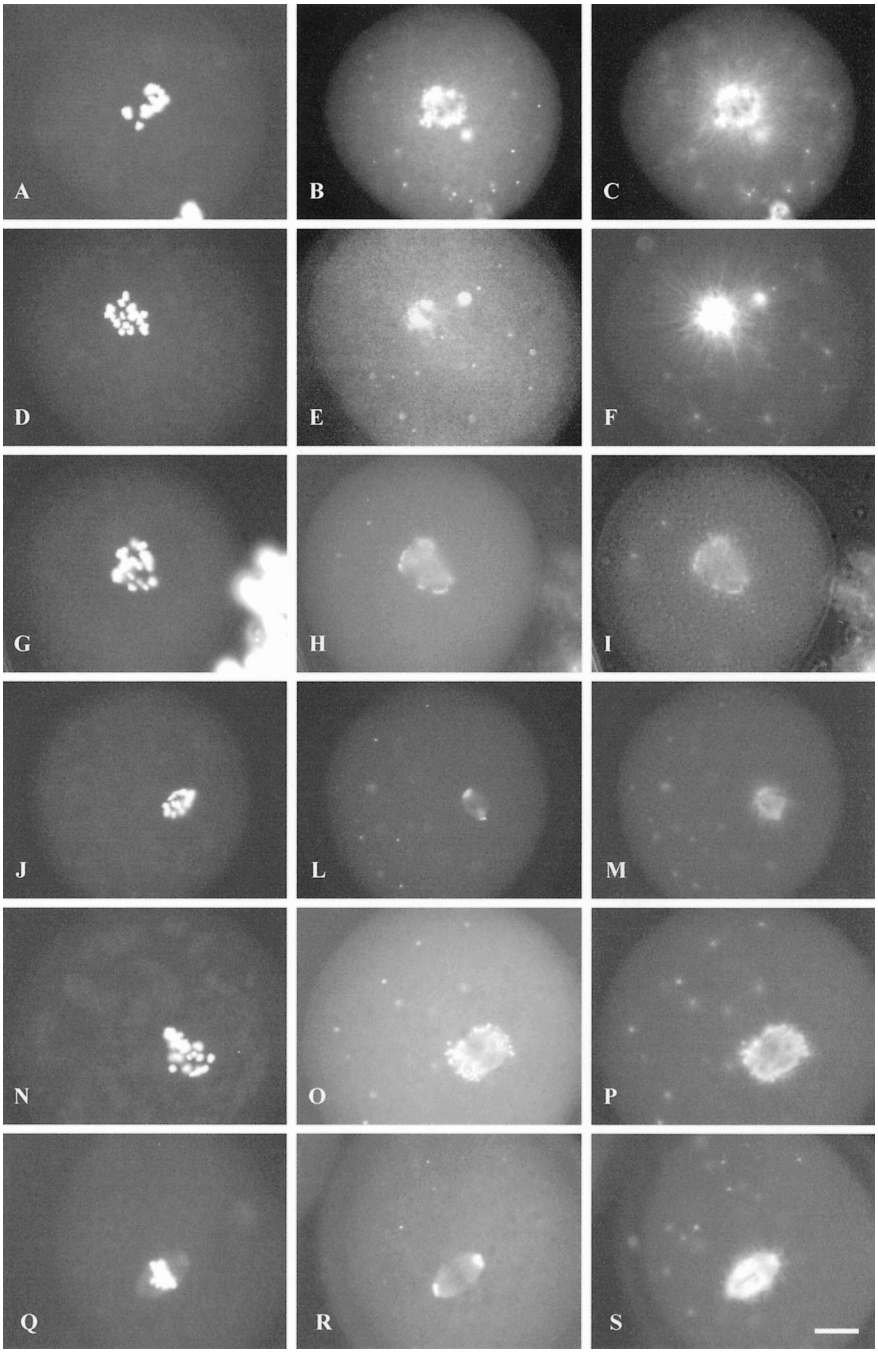

FIG. 7. Spindle morphogenesis in IVM (**A**–**C**, **G**–**I**, and **N**–**P**) and IVO oocytes (**D**–**F**, **J**–**M**, and **Q**–**S**) at 4, 6, and 8 h of meiotic progression. Correlative Hoechst 33258 (**A**, **D**, **G**, **J**, **N**, and **Q**), γ-tubulin (**B**, **E**, **H**, **L**, **O**, and **R**), and tubulin (**C**, **F**, **I**, **M**, **P**, and **S**) staining is shown at 4 (**A**–**F**), 6 (**G**–**M**), and 8 (**N**–**S**) h of meiotic progression. Note the more restricted distribution of γ-tubulin at 4 h of meiotic progression in IVO oocytes. Two restricted γ-tubulin foci at 6 and 8 h describe the spindle poles and entail formation of smaller spindles in IVO oocytes. Bar = 20 μm.

The regulation of the assembly of molecular components of the spindle poles and MTOCs may be of central importance during the process of oocyte maturation. During this asymmetric division, it is essential that molecular components of the spindle are properly arranged to allow balanced distribution of chromosomes and the asymmetric redistribution of other molecular factors to the oocyte and PB. This spatial regulation presumably serves to reduce meiotic aneuploidy and preserve polarized redistribution of factors in the oocyte.

Two issues related to the distinctions observed between IVM and IVO oocytes include the environmental conditions present during the course of maturation and whether methods employed for fixation and processing could influence structural organization of the spindle. Measures of spindle organization (Figs. 2 and 3), cytoplasmic MTOCs (Fig. 8), and PB content showed that IVO and IVO-N oocytes were identical. These results indicate that the properties of oocytes matured under physiological conditions bear similarity to those obtained following induced ovulation in CF-1 mice. A principal motivation for this study derives from the observation that defects during the process of meiotic maturation have often been cited as contributing to loss of developmental potential [30, 31]. To establish a baseline for future studies aimed at defining optimal IVM conditions, we employed only cumulus-oocyte complexes (COCs) from Graafian follicles obtained from eCG-primed mice and matured these oocytes under basal conditions in which cumulus expansion was not induced by hormone supplementation. It is likely that a fraction of the COCs used in this study are derived from Graafian follicles that would not have ovulated during a spontaneous or induced cycle,

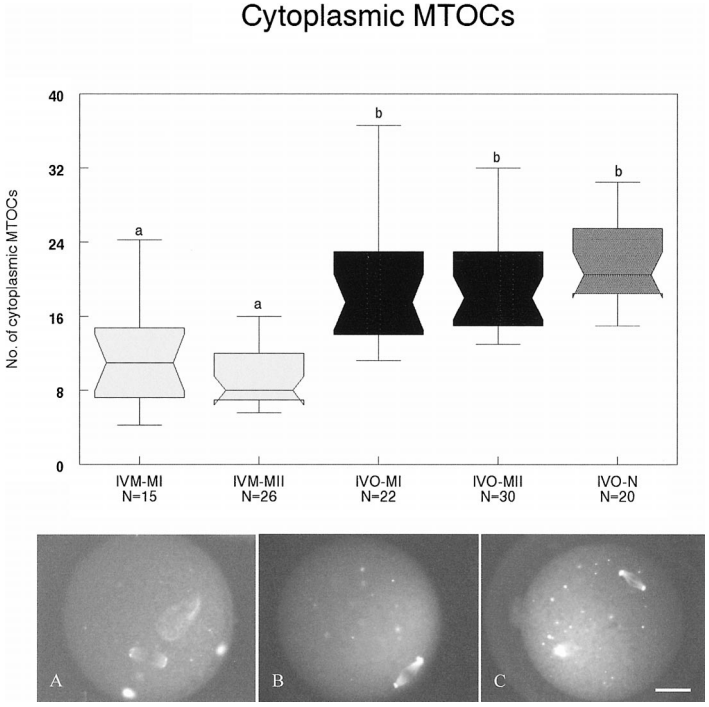

FIG. 8. Notched box plots demonstrate a near doubling of cytoplasmic MTOCs in IVO and IVO-N oocytes when compared with IVM oocytes as detected by γ-tubulin staining. The number of cytoplasmic MTOCs in IVO-N oocytes is similar to that observed in IVO oocytes. N represents numbers of oocytes analyzed for each meiotic stage. Different letters represent significant differences obtained across oocyte categories using nonparametric Kruskal-Wallis and Mann-Whitney tests ($P < 0.05$). Inserts represent M-II profiles of IVM (**A**), IVO (**B**), and IVO-N (**C**) oocytes labeled for γ-tubulin and used in the analysis of MTOC counts. Bar = 20 μm.

and thus the broader range of kinetic and structural changes reported in IVM oocytes may be attributable to heterogeneity in follicular origin and meiotic competence or failure to induce maturation with appropriate supplements. Nevertheless, the conditions used for IVM establish a frame of reference for comparison with the more consistent phenotypes we report for oocytes retrieved after natural or induced ovulations. To our knowledge, this is the first attempt to carefully characterize the IVO and IVM phenotype in any mammalian species.

The second issue raised by our studies pertains to the methods used to evaluate differences in spindle morphology. Mouse oocytes have long been recognized to exhibit a characteristic barrel-shaped spindle in both ultrastructural and immunofluorescence studies on IVM material [25, 32–34]. A transformation from meiotic anastral barrel-shaped spindles to mitotic spindles with pointed poles has been noted in prior studies on ovulated oocytes and embryos in the mouse [25, 34]. Our findings that in the mouse IVO oocyte spindles are small with characteristically pointed poles especially at M-II (Figs. 3–5) place into question the significance of variations in meiotic spindle morphology with respect to the different methodologies used for sample preparation. Close inspection of strategies used in other laboratories points to methodological differences that may underlie this issue, including 1) removal of the zona pellucida by acid-tyrodes or proteases, 2) extraction of oocytes with detergent prior to fixation, and 3) the use of fixatives other than formaldehyde. Although it is not within the purview of this paper to fully resolve how technical factors influence mouse oocyte meiotic spindle structure, support for the significance of our results derives from several lines of evidence, including 1) our demonstration of IVO and IVM spindle distinctions when the deuterium oxide and taxol, exogenous MT stabilizers used in our fixative, are removed from fixation solutions (unpublished results), 2) a comparison of five distinct mouse strains has consistently shown IVO and IVM oocyte differences in spindle shape identical to those reported here (Ibanez et al., manuscript in preparation), and 3) imaging using the pol-scope [35] and live fluorescence imaging of spindle MTs [36] have revealed a more pointed but still anastral phenotype in oocytes from various mouse lines, suggesting that methods of specimen preparation influence spindle structure. Among the remaining and more pressing questions of immediate relevance to understanding how oocyte quality is established are what mechanisms ensure the global management and utilization of cellular resources laid down during oogenesis and how these mechanisms are adjusted during remodeling of the oocyte cytoskeleton associated with meiotic maturation.

Variations in meiotic spindle structure and function have been observed recently in a number of genetic models that may be relevant to our understanding of the origins of meiotic aneuploidy in mammalian oocytes [37]. With respect to the hormonal environment to which oocytes are exposed during pre- and periovulatory stages of follicle development, in addition to spindle structure alterations IVO oocytes exhibit increased numbers of MTOCs and consistently smaller PBs compared with IVM oocytes. These extremes in phenotype are apparent in oocytes matured in a physiologically balanced hormonal milieu (IVO) or one lacking the complexity of hormonal signaling that typically occurs during ovulation. As shown by Hodges et al. [38], transgenic mice bearing elevated gonadotropins produce oocytes that exhibit meiotic spindle defects and heightened levels of meiotic aneuploidy. Moreover, mice bearing targeted deletions of GDF-9 [39] or connexin-37 [40] are hypogonadal and hypergonadotropic and similarly yield oocytes with severe meiotic spindle anomalies. Thus, hormonal conditions imposed on oocytes during early stages of follicle development are likely to influence the assembly and function of the meiotic spindle and are likely relevant to the increase in meiotic aneuploidy associated with maternal aging [41, 42]. Age-related or oocyte intrinsic factors also seem to critically establish meiotic spindle integrity in several mouse models. For example, functional telomeres appear to be required for meiotic spindle assembly in telomerase-deficient mice [43]. Loss of checkpoint control in mice homozygous for a targeted mutation of MLH1 also leads to abnormal spindle organization [44]. Mice bearing a targeted deletion of formin-2 exhibit failure of M-I due to the loss of spindle anchoring to the oocyte cortex that results in an inability to extrude the first PB [45].

A valuable genetic model for understanding the relationship between meiotic cell cycle control and spindle function are mice bearing a targeted deletion of c-mos or the Lt/Sv strain of mice. The c-mos −/− oocytes form pointed meiotic spindles that fail to migrate to the oocyte cortex, lack cytoplasmic MTOCs, and tend to form enlarged PBs, properties prompting speculation that these seemingly disparate phenomena coordinate karyokinesis with cytokinesis [36, 46, 47]. One common manifestation of c-mos loss is failure to regulate M-II arrest, resulting in parthenogenic activation as seen in c-mos −/− oocytes and oocytes from the Lt/Sv mouse strain. Loss of cytoplasmic MTOCs and the appearance of long pointed M-I spindles [47, 48] suggest that a relationship exists between spindle morphology and

MTOCs. We speculate that this c-mos-deficient phenotype yields pointed spindles because of the unavailability of γ-tubulin MTOCs; thus, barrel-shaped spindles formed after IVM result from the incorporation of multiple MTOCs during spindle assembly [12] (Fig. 7), whereas during IVO these foci have restricted access to the forming spindle because they may remain anchored to the oocyte cortex. This hypothesis receives support from our previous studies showing that γ-tubulin accumulation in meiotic spindles of IVM oocytes corresponds to the barrel-shape phenotype and reduction in cortical γ-tubulin foci. Coupled with the observations that IVM oocytes are metabolically compromised [49] and translationally inefficient [50], it seems likely that deficiencies in c-mos/mitogen-activated protein kinase (MAPK) pathway may underlie some of the distinctions we report here. Because MAPK is localized to spindle poles and MTOCs [51], the translation of c-mos mRNA may be inefficiently manifest during suboptimal conditions of IVM [52], resulting in barrel-shaped spindles, decreased number of cytoplasmic MTOCs, and large PBs. Synthesis and retention of functional MAPK in the cortex may restrict availability of γ-tubulin to the forming spindle, resulting in the smaller spindle sizes and limited size of the PB, which would be consistent with the increased number of cytoplasmic MTOCs and smaller PBs observed in IVO oocytes. The fact that IVO oocytes exhibit pointed spindles with focused localization of γ-tubulin at the spindle poles may reflect the fact that the utilization of γ-tubulin is more efficiently regulated during IVO than during IVM. Thus, many molecules, including γ-tubulin, are altered during IVM, and the causes and impact of each of these on developmental competence needs to be understood. More precisely, whether the c-mos/MAPK pathway establishes and maintains the spatial patterning of γ-tubulin and other vital maternal resources remains to be determined but should provide an important avenue for future studies on the determinants of oocyte quality. Besides critical cell cycle and spindle regulators (γ-tubulin, c-mos), a more global impact on metabolic efficiency may also underlie the differences uncovered presently between IVO and IVM oocytes.

The orchestration of karyokinesis and cytokinesis during the final stages of oogenesis is vital for egg activation and preimplantation embryonic development. Interactions between meiotic spindle components and the cortical actin cytoskeleton of oocytes must mediate the transition from a meiotic to mitotic phenotype, and candidate genes such as *formin-2* [45] and *c-mos* [46, 47] have been identified. Hatch and Capco [53] have suggested that the activation of cortically localized MAPK requires correct spatial positioning of calcium/calmodulin-dependent kinase II to effect the completion of meiosis and entry into embryonic interphase.

Establishing the precise roles for signaling intermediates, the cytoskeleton, and cell cycle regulators during meiotic progression in vivo will improve conditions for IVM of mammalian oocytes and should lead to a better understanding of the determinants of oocyte quality.

ACKNOWLEDGMENTS

We thank Dr. Qinsheng Gao for the provision of pericentrin antibodies and Dr. Elena Ibanez and Patricia Rodrigues for their helpful suggestions concerning the manuscript. We especially thank Dr. Catherine Combelles for her continued advice and critical insights that inspired this study and for important suggestions during manuscript preparation.

REFERENCES

1. Eppig JJ, O'Brien MJ. Comparison of preimplantation developmental competence after mouse oocyte growth and development in vitro and in vivo. Theriogenology 1998; 49:415–422.
2. Mermillod P, Oussaid B, Cognie Y. Aspects of follicular and oocyte maturation that affect the developmental potential of embryos. J Reprod Fertil Suppl 1999; 54:449–460.
3. Moor R, Dai Y. Maturation of pig oocytes in vivo and in vitro. Reprod Suppl 2001; 58:91–104.
4. Trounson A, Anderiesz C, Jones G. Maturation of human oocytes in vitro and their developmental competence. Reproduction 2001; 121: 51–75.
5. Edwards RG. Maturation in vitro of mouse, sheep, cow, pig, rhesus monkey and human ovarian oocytes. Nature 1965; 208:349–351.
6. Pincus G, Enzmann V. The comparative behavior of mammalian eggs in vivo and in vitro. J Exp Med 1935; 62:665–675.
7. Sutton ML, Gilchrist RB, Thompson JG. Effects of in-vivo and in-vitro environments on the metabolism of the cumulus-oocyte complex and its influence on oocyte developmental capacity. Hum Reprod Update 2003; 9:35–48.
8. Telfer EE. In vitro models for oocyte development. Theriogenology 1998; 49:451–460.
9. Bousquet D, Twagiramungu H, Morin N, Brisson C, Carboneau G, Durocher J. In vitro embryo production in the cow: an effective alternative to the conventional embryo production approach. Theriogenology 1999; 51:59–70.
10. Barnes F, Endebrock M, Looney C, Powell R, Westhusin M, Bondioli K. Embryo cloning in cattle: the use of in vitro matured oocytes. J Reprod Fertil 1993; 97:317–320.
11. De Rycke M, Liebaers I, Van Steirteghem A. Epigenetic risks related to assisted reproductive technologies: risk analysis and epigenetic inheritance. Hum Reprod 2002; 17:2487–2494.
12. Combelles CM, Albertini DF. Microtubule patterning during meiotic maturation in mouse oocytes is determined by cell cycle-specific sorting and redistribution of gamma-tubulin. Dev Biol 2001; 239:281–294.
13. Plancha CE, Albertini DF. Hormonal regulation of meiotic maturation in the hamster oocyte involves a cytoskeleton-mediated process. Biol Reprod 1994; 51:852–864.
14. Combelles CM, Cekleniak NA, Racowsky C, Albertini DF. Assessment of nuclear and cytoplasmic maturation in in-vitro matured human oocytes. Hum Reprod 2002; 17:1006–1016.
15. Liu H, Krey LC, Zhang J, Grifo JA. Ooplasmic influence on nuclear function during the metaphase II-interphase transition in mouse oocytes. Biol Reprod 2001; 65:1794–1799.
16. Bao S, Obata Y, Carroll J, Domeki I, Kono T. Epigenetic modifications necessary for normal development are established during oocyte growth in mice. Biol Reprod 2000; 62:616–621.
17. DeSciscIolo C, Wright DL, Mayer JF, Gibbons W, Muasher SJ, Lanzendorf SE. Human embryos derived from in vitro and in vivo matured oocytes: analysis for chromosomal abnormalities and nuclear morphology. J Assist Reprod Genet 2000; 17:284–292.
18. Nogueira D, Staessen C, Van de Velde H, Steirteghem AV. Nuclear status and cytogenetics of embryos derived from in vitro-matured oocytes. Fertil Steril 2000; 74:295–298.
19. Champlin AK, Dorr DL, Gates AH. Determining the stage of the estrous cycle in the mouse by the appearance of the vagina. Biol Reprod 1973; 8:491–494.
20. Messinger SM, Albertini DF. Centrosome and microtubule dynamics during meiotic progression in the mouse oocyte. J Cell Sci 1991; 100: 289–298.
21. Kilmartin JV, Wright B, Milstein C. Rat monoclonal antitubulin antibodies derived by using a new nonsecreting rat cell line. J Cell Biol 1982; 93:576–582.
22. Maro B, Kubiak J, Gueth C, De Pennart H, Houliston E, Weber M, Antony C, Aghion J. Cytoskeleton organization during oogenesis, fertilization and preimplantation development of the mouse. Int J Dev Biol 1990; 34:127–137.
23. Carabatsos MJ, Combelles CM, Messinger SM, Albertini DF. Sorting and reorganization of centrosomes during oocyte maturation in the mouse. Microsc Res Tech 2000; 49:435–444.
24. Doxsey SJ, Stein P, Evans L, Calarco PD, Kirschner M. Pericentrin, a highly conserved centrosome protein involved in microtubule organization. Cell 1994; 76:639–650.
25. Maro B, Howlett SK, Webb M. Non-spindle microtubule organizing

centers in metaphase II-arrested mouse oocytes. J Cell Biol 1985; 101: 1665–1672.
26. Miyoshi K, Rzucidlo SJ, Pratt SL, Stice SL. Improvements in cloning efficiencies may be possible by increasing uniformity in recipient oocytes and donor cells. Biol Reprod 2003; 68:1079–1086.
27. Gardner RL. Specification of embryonic axis begins before cleavage in normal mouse development. Development 2001; 128:839–847.
28. Albertini DF. Regulation of meiotic maturation in the mammalian oocyte: interplay between exogenous cues and the microtubule cytoskeleton. Bioessays 1992; 14:97–103.
29. Rugh R. The Mouse—Its Reproduction and Development. Minneapolis: Burgess; 1968:32–35.
30. Schroeder AC, Eppig JJ. The developmental capacity of mouse oocytes that matured spontaneously in vitro is normal. Dev Biol 1984; 102:493–497.
31. Schroeder AC, Downs SM, Eppig JJ. Factors affecting the developmental capacity of mouse oocytes undergoing maturation in vitro. Ann N Y Acad Sci 1988; 541:197–204.
32. Szollosi D, Calarco P, Donahue RP. Absence of centrioles in the first and second meiotic spindles of mouse oocytes. J Cell Sci 1972; 11: 521–541.
33. Wassarman PM, Fujiwara K. Immunofluorescent anti-tubulin staining of spindles during meiotic maturation of mouse oocytes in vitro. J Cell Sci 1978; 29:171–188.
34. Schatten G, Simerly C, Schatten H. Microtubule configurations during fertilization, mitosis, and early development in the mouse and the requirement for egg microtubule-mediated motility during mammalian fertilization. Proc Natl Acad Sci U S A 1985; 82:4152–4156.
35. Liu L, Trimarchi JR, Oldenbourg R, Keefe DL. Increased birefringence in the meiotic spindle provides a new marker for the onset of activation in living oocytes. Biol Reprod 2000; 63:251–258.
36. Verlhac MH, Lefebvre C, Guillaud P, Rassinier P, Maro B. Asymmetric division in mouse oocytes: with or without Mos. Curr Biol 2000; 10:1303–1306.
37. Champion MD, Hawley RS. Playing for half the deck: the molecular biology of meiosis. Nat Cell Biol 2002; 4(suppl):s50–s56.
38. Hodges CA, Ilagan A, Jennings D, Keri R, Nilson J, Hunt PA. Experimental evidence that changes in oocyte growth influence meiotic chromosome segregation. Hum Reprod 2002; 17:1171–1180.
39. Carabatsos MJ, Elvin J, Matzuk MM, Albertini DF. Characterization of oocyte and follicle development in growth differentiation factor-9-deficient mice. Dev Biol 1998; 204:373–384.
40. Carabatsos MJ, Sellitto C, Goodenough DA, Albertini DF. Oocyte-granulosa cell heterologous gap junctions are required for the coordination of nuclear and cytoplasmic meiotic competence. Dev Biol 2000; 226:167–179.
41. Volarcik K, Sheean L, Goldfarb J, Woods L, Abdul-Karim F, Hunt PA. The meiotic competence of matured human oocytes is influenced by donor age: evidence that folliculogenesis is compromised in the reproductively aged ovary. Hum Reprod 1998; 13:154–160.
42. Battaglia DE, Goodwin P, Klein NA. Influence of maternal age on meiotic spindle assembly in oocytes from naturally cycling women. Hum Reprod 1996; 11:2217–2222.
43. Liu L, Blasco MA, Keefe DL. Requirement of functional telomeres for metaphase chromosome alignments and integrity of meiotic spindles. EMBO Rep 2002; 3:230–234.
44. Woods LM, Hodges CA, Baart E, Baker SM, Liskay M, Hunt P. Chromosomal influence on meiotic spindle assembly: abnormal meiosis I in female Mlh1 mutant mice. J Cell Biol 1999; 145:1395–1406.
45. Leader B, Lim H, Carabatsos MJ, Harrington A, Ecsedy J, Pellman D, Maas R, Leder P. Formin-2, polyploidy, hypofertility and positioning of the meiotic spindle in mouse oocytes. Nat Cell Biol 2002; 4: 921–928.
46. Choi T, Fukasawa K, Zhou R, Tessarollo L, Borror K, Resau J, Vande Woude GF. The Mos/mitogen-activated protein kinase (MAPK) pathway regulates the size and degradation of the first polar body in maturing mouse oocytes. Proc Natl Acad Sci U S A 1996; 93:7032–7035.
47. Verlhac MH, Kubiak JZ, Weber M, Geraud G, Colledge WH, Evans MJ, Maro B. Mos is required for MAP kinase activation and is involved in microtubule organization during meiotic maturation in the mouse. Development 1996; 122:815–822.
48. Albertini DF, Eppig JJ. Unusual cytoskeletal and chromatin configurations in mouse oocytes that are atypical in meiotic progression. Dev Genet 1995; 16:13–19.
49. Combelles CM, Albertini DF. Assessment of oocyte quality following repeated gonadotropin stimulation in the mouse. Biol Reprod 2003; 68:812–821.
50. Schultz RM, LaMarca MJ, Wassarman PM. Absolute rates of protein synthesis during meiotic maturation of mammalian oocytes in vitro. Proc Natl Sci U S A 1978; 75:4160–4164.
51. Verlhac MH, de Pennart H, Maro B, Cobb MH, Clarke HJ. MAP kinase becomes stably activated at metaphase and is associated with microtubule-organizing centers during meiotic maturation of mouse oocytes. Dev Biol 1993; 158:330–340.
52. Eichenlaub-Ritter U, Peschke M. Expression in in-vivo and in-vitro growing and maturing oocytes: focus on regulation of expression at the translational level. Hum Reprod Update 2002; 8:21–41.
53. Hatch KR, Capco DG. Colocalization of CaM KII and MAP kinase on architectural elements of the mouse egg: potentiation of MAP kinase activity by CaM KII. Mol Reprod Dev 2001; 58:69–77.